Geological Research using Electronic Markers

Design of a signal processing system for chipless RFID

TU Delft

Geological Research using Electronic Markers

Design of a signal processing system for chipless RFID

Bachelor Graduation Project
at the Delft University of Technology.

Project duration:	April 1, 2019 – July 6, 2019	
Supervisor:	Dr. ir. G. de Graaf	
Proposer:	Dr. M.E. Donselaar	
Collaborators:	D. de Groot	(4607414)
	E.R. van der Meijs	(4567528)

TU Delft

Abstract

In this thesis, the implementation of a passive, chipless, frequency coded RFID detection system for bed-load transport studies is proposed. The proposed tag will be deployed in the semi-arid Río Colorado, Bolivia with the aim to develop quantitative sediment transport models that relate transport to grain size. Different algorithms are explored and implemented in Matlab and measurement results are discussed.

Preface

Sediment transport studies are essential to understand how natural structures are created, modified or destroyed. As a part of these studies, integrated quantitative models of sediment routing systems are made. The tracking and tracing of individual sediment particles is of key importance in the construction of these models. Since its existence, research has been conducted in a variety of ways. In the last two decades, the use of Radio-Frequency Identification (RFID) technology has become more viable and preferable for the ability to individually distinguish between tracers. However, the size of current RFID tags limits the research to tracking only larger sized sediment. The aim of the Bachelor Graduation Project (BAP) is to develop a system that would allow the further down scaling of a tag to eventually be able to gather quantifiable measurements on the transport parameters of sand-like sediment. The product is initially developed to aid in the evaluation of the pristine Rio Colorado sediment-routing system in the semi-arid, sparsely-vegetated Altiplano Basin of Bolivia in a joint research between KU Leuven and Delft University of Technology.

Firstly, we would like to thank Dr. M.E. (Rick) Donselaar for proposing this project. Dr. Donselaar has given us great insights into the importance and applications of sediment tracing studies, which has proved to be of great importance for this project. Secondly, we would like to thank dr.ir. G. de Graaf for his supervision during this thesis. His guidance has helped us immensely in structuring the project. We would also like to thank ir. P.J. (Pascal) Aubry for helping us set up UWB measurement setup. Morevover, Prof. Alexander Yarovoy is appreciated for his effort in structuring the problem and assisting us with possible solutions.

Contents

1 Introduction

Since the beginning of time, rivers have shaped landscapes in extraordinary ways. To understand how rivers form and function, bedload transport studies are of key importance. Data collected from these studies can be used to further develop general sediment transport models. The goal of these models is to eventually be able make statements about the sediment transport of an arbitrary river. Changes in sediment quantity and quality can not only have effect on the environment, but also on social and economic systems [1]. Examples of this include research on the behaviour of the Kulim River in Malaysia, which floods frequently [2].

To construct quantitative integrated models for sediment routing systems, the ability to track and trace individual sediment particles in space and time is essential. Serious tracking studies started with the tracking of radioactively tagged particles in the 1950s. This method cannot be used in most situations because of health and safety issues. Other methods include the use of fluorescent glass and magnetic material. The fluorescent glass is able to be detected at range using UV light and the particles are able to be sized down to 44 μm. It has however only been used in simulations on laboratory scale [3]. The magnetic material is arguably more cumbersome requiring soil samples both before and afterwards, as well as knowledge of loss of magnetic characteristics of the material used [4]. Neither of the methods mentioned above have the option to deploy individually distinguishable tags.

In the last two decades, a growing number of researchers made use of radio frequency identification technology to research bedload transport [5]. This method is advantageous as it allows tracers that are relatively cheap, durable and can be distinguished by unique codes [6]. The unique code of RFID tags allows to track individual displacement of particles, which allows for more complex modelling of river systems.

RFID systems consist of a reader or scanner and a transponder or tag. When exited, the tag transfers data to the reader. This can be done in two ways: transferring through a magnetically coupled circuit located in the near field, or using a send and listen method with the tag and reader placed in each others far field region [7]. The currently used systems are low-frequency tags working in the near field, achieving ranges up to about 40 centimetres [6]. The tags used are passive and contain a chip which is harvesting the energy from the electromagnetic waves from the reader. When sufficient energy is harvested, it is used to power the on board integrated circuit which in turn will send out an electromagnetic (EM) signal which, when received, can be used to identify the tag. The typical size of these tags is about $20-30$ millimetres [6]. Similar RFID technologies are used for different research subjects. For example, to study the behaviour of bees. In this case, RFID tags have been placed on the bees with the readers placed at the entrances of the hive [8]. Again the chips where passive and with a chip, sized $3.1 \times 1.6 \times 0.5$ millimetres, achieving a reading range of about 5 millimetres.

This thesis focuses on the development of an RFID system used for sediment research in the Río Colorado, Bolivia [9]. The Río Colorado is special in the regard that it is a very simple river to model. It has one source and one sink, and mouths into a shallow salt lake. The river is semi-arid, as many rivers are on this globe and the region has little to no vegetation, which simplifies the modelling of rain water. Sediment research calls for uniquely identifiable tags that reach the size of sand grains. Current technology is either uniquely identifiable

or as small as sand, but not both. On the same token, technology should remain cheap and durable. The gap in this technology poses limits to sediment transport models that can be constructed, as is the case in rivers around the world.

This poses the following design challenge:

Design uniquely identifiable tracers that behave like sand grains through a riverbed.

It is argued that the solution is a chipless, passive RFID system using Vivaldi antennas for detection and digital signal processing technology in the frequency domain in combination with a global positioning system (GPS). This particular thesis has its focus on the design of the digital signal processing which will be implemented in Matlab. For the design of the other system components, one should consult the work of Kraaijeveld, M. and De Gruijl or Roos, S. and Postma M.A.

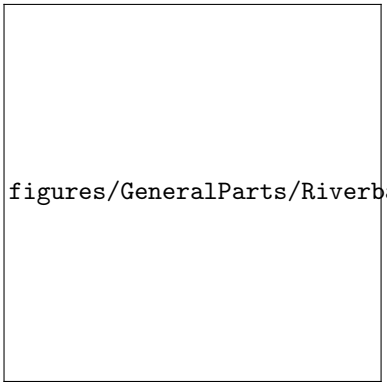

(a) Grass-covered bank in the upstream area

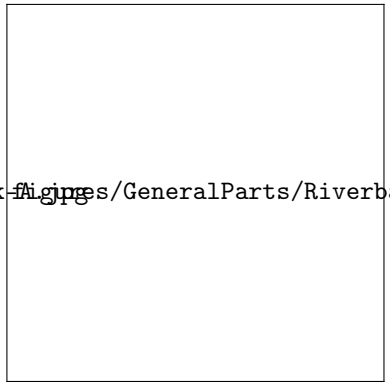

(b) Non-vegetation bank in the downstream area

Figure 1.1: Upper coastal plain [9]

2

System requirement analysis

With the design question:

> Design uniquely identifiable tracers that behave like sand grains through a riverbed.

only a broad goal for this project is established. No concrete requirements are apparent. With the aim to solidify and specify the objective a couple of meetings with Rick Donselaar were scheduled to discuss his needs regarding sediment tracing and the nature of the underlying problem. From this point a success scenario was written, from which direct functional and non-functional requirements can be derived following the template by Bahill and Dean [10].

Use case name: Geological research using Electronic Markers

Main success scenario

1. Distinct tags are distributed over the river bedding at known locations.
2. The rain season starts and the tags drift downstream behaving exactly like the sediment they were placed in.
3. The rain season passes and the river dries up.
4. The measurement device is attached to the vehicle.
5. The vehicle moves at low speed through the river bedding.
6. Tags are located and their respective locations are placed in a spreadsheet
7. The locations are analysed by the researcher.
8. Every tag may stay in the river and is able to be detected again for further analysis after next rain season.

Functional requirements

F1. The tracers should be detected wirelessly.

F2. The tracers should be uniquely identifiable up to a 100 devices.

F3. The tracers should behave as sand grains on a riverbed.

F4. The tracers should be able to withstand salty water.

F5. The tracers should be detectable from a vehicle.

F6. The tracers should be detectable from a minimum of 40 cm while buried up till 5 cm in sand.

F7. The measurement setup should be transportable through the riverbed.

F8. The measurement system has to function in a temperature range between -10 and 40 degrees Celsius.

F9. The tracers should withstand temperatures in a range -20 and 50 degrees Celsius.

Non-functional requirements

N1. The system should present collected locations in a straightforward way.

N2. The tags should be recoverable or non-harmful to the environment.

N3. The system should be save for people to work around.

N4. The system should comply with relevant organisational and governmental regulations.

3

System Design

On the basis of this project, three theses will be written. To understand how each thesis will be structured, preliminary design choices have to be made. In this chapter, these design choices are substantiated. First, a short recap will be made on why an RFID system was chosen. Then, the choices and considerations in RFID systems will be explained. Subsequently, a number of possible designs will be laid out, based on their working principle, an exemplar implementation, the expected performance and its feasibility within the context of the project. Finally, a design choice will be made and its general system will be further explained. This system is split into three subsystems, which will each be one thesis.

3.1. Types of technology

A number of different sediment tracing methods are currently used to track sand-like material. They are generally divided into two groups [3].

1. Labelled (coated) natural particles
2. Labelled synthetic particles

Associated with the first group are for instance natural particles labelled with fallout radionuclides, fluorescent paints and fingerprinting techniques [4]. Due to their primitive nature they lack the ability to be individually distinguishable. With advancements in technology the production of synthetic particles became feasible. This allowed for the use of materials that facilitate the detection of the tracers more consistently. The common tracers used in this category are rare earth elements (REE) tracers, magnetic substances and polystyrene plastics [3]. These types of traces do have the ability to be distinguishable between sets using chemical processes that are rather cumbersome and require soil samples [4]. More recently, RFID has also been used to track larger sediment particles, e.g. boulders, cobbles and pebbles [6].

3.2. Choice for RFID

There is a significant difference between the use case of previously used RFID tracers and the one of the design problem described in this thesis. The locations of the tags in Bolivia are only measured outside of the rainy season, when the riverbed has run dry. As a result the use of EM waves becomes an option because attenuation through water no longer poses an issue. RFID technology that allows for individual identification has already been used to research group behaviour of bees. However, the devices used in this research have a relatively small detection range of about 5 mm [8].

Compared to the previously used technologies RFID seems to be more in line with the requirements. Therefore, the first major decision is to pursue detection of the particle based on RFID technology.

3.3. RFID technology

Since the choice has fallen on RFID in section 3.2, a choice needs to made which type of RFID coding will be used. This coding type will determine all specifications and parameters for all subgroups, and is therefore of key importance. This section will describe the various RFID technologies which were under consideration.

3.3.1. Active and passive designs

In RFID tracking systems, there are two major technologies that can be defined: passive and active tracking. Passive RFID tags have no internal power source. Active RFID tags are battery-powered and are able to broadcast their own signal continuously. They are more often used for continuous tracking, have a long read range and are more expensive. Passive tags are cheap and small, but their range is limited, since no extra energy from an internal source can be drawn to send back a stronger signal to the reader [11].

To design the RFID system, a few requirements were taken into account. First of all, the tag should be as small as possible, preferably as small as grains of sand. This puts enormous stress on the design of a battery system if an active RFID system should be realised. Secondly, the price is taken into account. The tags should be as cheap as possible, because they are deployed in large numbers. Passive tags are cheaper than active tags, since their design is often simpler. Thirdly, passive tags can last a lifetime without a battery, depending on the wear and tear. This is not the case for active tags. Since the sediment research is done over several years, it is important that the tags can operate for several seasonal cycles.

3.3.2. Chipped or chipless design

A passive tag can be implemented in two ways: with or without an embedded chip. The chipless tags are made by creating conductive structures on a substrate in such a way that it will generate a time- or frequency domain signature when it is exited with RF energy [12]. Integrated circuit (IC) based systems mostly use backscattering by changing the impedance of their antennas. The advantages of chipless systems is that production is much more simple than IC production and thus less costly. But after production the encoded information can not be changed anymore. Systems based on resonant structures also do not need a separate antenna which can provide robustness and size advantages. Chip based systems have the advantage that they can provide more complex functions than just identification, by for example implementing a time delay between receiving the interrogation signal and their response or encryption of the contained data.

3.3.3. Time and Frequency Coding

Chipless tags are often categorised into two types [13]. The tags in the first category are either retransmission or time-domain reflectometry (TDR) chipless RFID tags. This category of tags uses encoding in the time domain. Data is not encoded in the antennas itself. Instead, the signal is first received by an antenna, then the signal is transformed or simply delayed, thereafter retransmitted. The important data is often encoded by positioning parasitic elements along a transmission line to create reflections at precise moments.

The tags in the second category are either scattering or millimeter-wave (mmW) image-based chipless RFID tags. In these tags, the antenna itself is a resonating element which causes peaks or dips in the frequency spectrum of the received signal. This type of encoding mainly uses the UWB band (3.1-10.6 GHz), which has significant restrictions on the transmitting power.

The tag is required to have a high quality factor, which means its peak(s) have a very narrow bandwidth, such that it resonates at very specific frequencies. The quality factor also influences how long the tag keeps resonating. A high quality factor gives the opportunity to measure the signal after the initial reflection has been received.

Temporal coded tags often have longer reading ranges than spectrum coded tags. The spectrum coded tags use high frequencies, which limits their range. However, spectrum coded tags have higher information densities, which allow them to reach smaller sizes for the same information stored [13].

3.4. RFID link

Every RFID system contains by definition an EM link between the tag and the transponder. Information is sent over this link, but not all signal power will reach the receiver. Moreover, noise will be added to the system and reflected signals can interfere with the signal or even saturate the receiver. A better understanding of these phenomena will be given in this section.

There is a difference between the so-called near-field and far-field RFID technologies. In low-frequency near-field technologies, waves do not actually propagate but only exist as a reactive field near the transmitter. By

modulating this reactive field with the tag, the transmitter can directly 'feel' the modulation and can communicate with the tag. However, the tags to be used for this project must be very small, requiring high-frequency EM waves. For this reason, a far-field RFID system needs to be implemented and the calculations in this section assume far-field propagation.

3.4.1. Signal power

In a far-field RFID system, the transponder will send a signal to a tag, which will respond. Because the antennas are not made to be perfectly directional as the exact location of the markers is not known, this signal power will spread out which wastes part of the energy. These power transfer characteristics will be described in this subsection. The RFID system can be modelled as a radar system or a free space transmission link. When an electronic marker system is based on a reflection caused by the marker, the system can be modelled as a radar system. When a system is based on a re-transmission of a (manipulated) transmitted signal, the system can be modelled as a free space transmission link.

Radar system

To calculate the received power reflected by an object, the transmitted power density must be calculated first. The power of an isotropic antenna spreads out over a sphere. However, the antenna is not isotropic and transmits more power in a certain direction. This is called the gain G. Including this gain, the power density at a distance R transmitted by an antenna can be calculated with Equation 3.1.

$$S_{transmitted} = G \cdot \frac{P_{transmitted}}{4\pi \cdot R^2} \quad [\mathrm{W\,m^{-2}}] \quad (3.1)$$

With the power density, the reflected power can be calculated using the reflective area of the object. The reflective area depends on the physical area of the object. However, the reflective area of the object is also material and frequency dependent. The reflective area in radar theory is described by the radar cross-Section (RCS). Using the RCS σ, the reflected power can be calculated using Equation 3.2.

$$P_{reflected} = \sigma \cdot G \cdot \frac{P_{transmitted}}{4\pi \cdot R^2} \quad [\mathrm{W}] \quad (3.2)$$

The reflected power is again spread out over a sphere and the power density will result in Equation 3.3.

$$S_{reflected} = \frac{P_{reflected}}{4\pi \cdot R^2} \quad [\mathrm{W\,m^{-2}}] \quad (3.3)$$

The received power is this time calculated by multiplying the power density with the effective area of the antenna. However, the effective area of the antenna is not equal to the physical area. The effective area of the antenna in radar theory is described by the effective aperture A_e. The received power is calculated using Equation 3.4

$$P_{received} = S_{reflected} \cdot A_e \quad [\mathrm{W}] \quad (3.4)$$

The effective aperture is not easy to determine for all antennas. However, the gain is known by simulation or measurement. The relation between the effective aperture and the gain of an antenna is given by Equation 3.5.

$$A_e = G \cdot \frac{\lambda^2}{4\pi} \quad [\mathrm{m^2}] \quad (3.5)$$

Combining Equation 3.2, Equation 3.4 and Equation 3.5 results in the radar equation, Equation 3.6. By filling in typical values for the quantities a ratio between the transmitted power and received power can be found.

$$P_{received} = \frac{P_{transmitted}}{(4\pi)^3 \cdot R^4} \cdot \sigma \cdot G^2 \cdot \lambda^2 \quad [\mathrm{W}] \quad (3.6)$$

Transmission link

To calculate the received power in case of a free space transmission link, the transmitted power density must be calculated first as well. This is the same as the transmission of the radar based system in Equation 3.1. The marker can be modelled as an antenna that receives power and then retransmits the power. The received power at the marker is calculated by multiplying the power density by the its effective area, which is done in Equation 3.7.

$$P_{received,tag} = A_{e,tag} \cdot G_{antenna} \cdot \frac{P_{transmitted}}{4\pi \cdot R^2} \quad [\mathrm{W}] \quad (3.7)$$

This retransmission is the same as the initial transmission and can be calculated using Equation 3.1 as well. The received power is again calculated by multiplying the power density with the effective area of the antenna. However, the antenna gain is known for the receiving antenna and Equation 3.5 can be substituted in order to get the Friis transmission equation for a double antenna link, see Equation 3.8.

$$P_{received,antenna} = \frac{P_{transmitted}}{(4\pi)^3 \cdot R^4} \cdot A_{e,tag} \cdot G^2_{antenna} \cdot \lambda^2 \quad \text{[W]} \tag{3.8}$$

3.4.2. Reflections

The environment in which the tags need to be detected is the dry riverbed of the Río Colorado in Bolivia. This riverbed mainly consists of dry sand, with grain sizes in the range of 0.1 - 0.4 mm [9]. The tags are on or slightly below the surface of the sand and the antennas can be close above this surface. On the boundary between these media with different electromagnetic properties is a difference in impedance. This difference will cause reflections when a wave hits the boundary. The amount of power reflected can be indicated using the reflection coefficient. The reflection coefficient can be calculated using the difference in impedance of the media with Equation 3.9.

For a normal incidence wave on a boundary between two low loss dielectrics, with $\mu_0 \approx \mu_1 \approx \mu_2$ the formula for the reflection coefficient can be rewritten using only the relative permittivity ϵ_r.

$$r = \frac{\eta_2 - \eta_1}{\eta_2 + \eta_1} = \frac{\sqrt{\frac{\mu_2}{\epsilon_2}} - \sqrt{\frac{\mu_1}{\epsilon_1}}}{\sqrt{\frac{\mu_2}{\epsilon_2}} + \sqrt{\frac{\mu_1}{\epsilon_1}}} = \frac{\sqrt{\epsilon_1} - \sqrt{\epsilon_2}}{\sqrt{\epsilon_1} + \sqrt{\epsilon_2}} = \frac{\sqrt{\epsilon_{air}} - \sqrt{\epsilon_{sand}}}{\sqrt{\epsilon_{air}} + \sqrt{\epsilon_{sand}}} \tag{3.9}$$

The permittivities for sand and air are listed in Table 3.1. Both media are nonmagnetic, meaning that their $\mu = \mu_0$. Finally, both media can be approximated as lossless: dry sand has a skin depth of several meters [14].

The reflected power is proportional to the square of the reflection coefficient r and can be calculated using Equation 3.10 with the data from above. The reflected power due to the boundary between air and sand is 5.5%.

$$R = |r|^2 = \left| \frac{\sqrt{\epsilon_{air}} - \sqrt{\epsilon_{sand}}}{\sqrt{\epsilon_{air}} + \sqrt{\epsilon_{sand}}} \right|^2 = \left| \frac{\sqrt{1} - \sqrt{2.6}}{\sqrt{1} + \sqrt{2.6}} \right|^2 = 0.055 = -12.6 \text{ dB} \tag{3.10}$$

Table 3.1: Electromagnetic characteristics of air and sand [14]

	Relative permittivity ϵ_r	**Relative permeability μ_r**
Air	1	1
Sand	2.6	1

Clutter

Besides the interface between the air and the sand, there will also be small air pockets within the sand. Therefore, the sand is a non-uniform medium. When these pockets are sized in the same order or larger compared to the wavelength, these will cause reflections as well. Multiple received reflections are called clutter. In a lab setup, the clutter is constant and can be calibrated out by making an initial reference measurement [15]. However, when driving around, this clutter is far from constant and this method can not be used.

Exactly calculating the effects of clutter is difficult, because the plane wave approximation cannot be used when the reflective surface is small and the structure of the sand in the river is not known.

Part of the clutter can be eliminated. This elimination is implementation dependent. A variety of solutions is described below.

Implementations that use an impulse response can eliminate clutter in the time domain. For example, undesired clutter further away from the tags are irrelevant and can be discarded by windowing the time domain signal. Since the undesired reflections travel a longer distance, by windowing the signal in time domain these reflections can be filtered away.

Tags can also use frequency domain separation to remove part of the clutter as well. An electronic marker that is based on a re-transmission of a signal can retransmit the signal in another frequency band. By adding a filter to the receiver, most clutter can be filtered out.

The clutter can also be eliminated by depolarisation. Many surfaces do not change the polarisation characteristics of an EM wave, which can be utilised to distinguish between reflections and tags. This solution obligates tags that are able to change the polarisation of the retransmitted waves in comparison to the incident waves. If the transmit and receive antenna are cross-polarised and have a good polarisation isolation, many reflections will not be received. A disadvantage of this is the loss in power when the polarisation is randomised.

3.4.3. Noise

The detection system contains various noise sources. An ideal antenna does not generate noise, it only receives noise from the environment. In the environment of the antenna are natural noise sources and man-made noise sources. For this project, the antenna should receive signals from the ground, therefore it is directed at the ground. However, the antennas are not perfectly directional and noise from other areas such as the sky are received too. The largest natural noise source in the sky is the thermal noise from the sun. Man-made noise sources are electromagnetic influences from nearby radiation sources. One example might be the ignition system of a petrol car [16], on which the antennas might get mounted. The noise that naturally occurs is thermal noise from objects in the antenna path. In this section, these naturally occurring noise contributions are calculated.

For the noise calculations, the antenna is considered to be directed to the ground with the sun exactly above it. These values are realistic for antennas with an opening angle of about 60 degrees. The main lobe, the direction in which the most power is emitted, is directed to the ground while the oppositely directed back lobe is directed to the sun. For the calculations it is assumed that the antenna gain of the main lobe is 2 and the back lobe 1.

The antenna opening aperture directed to the sun is approximately half a degree, as shown in Equation 3.11. The antenna gain at this angle can be considered constant and is equal to the back lobe gain.

$$\Theta_{sun} = 2 \cdot \arctan\left(\frac{R_\odot}{r_\oplus}\right) \approx 0.5^\circ \tag{3.11}$$

From this data, the noise temperature can be calculated using Equation 3.12.

$$T = \frac{1}{4\pi}\int_0^{2\pi}\int_0^{\pi} R(\theta,\phi)\,T(\theta,\phi)\sin(\theta)\,\mathrm{d}\theta\,\mathrm{d}\phi = \frac{1}{4\pi}\Big(2\pi\cdot 2\cdot T_{ground} + (1-\cos(\Theta_{sun}))\cdot T_{sun}\Big) \tag{3.12}$$

Since the localisation of the tags is not during summer, with a cooler climate in the target area [9], a ground temperature of 300 Kelvin was chosen. For the sun temperature, 10^5 K was chosen, which is an approximate long-term average for the sun temperature measured at 2.8 GHz [17]. Substituting the information in Equation 3.12 results in Equation 3.13.

$$T = \frac{1}{4\pi}\left(2\pi\cdot 2\cdot 300 + \left(1-\cos\left(\frac{0.5\pi}{180}\right)\right)\cdot 10^5\right) = 300 + 3.8 = 303.8\ \mathrm{K} \tag{3.13}$$

In Equation 3.13 can be seen that the noise from the ground has by far the largest noise contribution, and therefore the other natural noise sources can be neglected. With this temperature, the total noise power in the complete UWB-band from approximately 3 GHz to 10 GHz is calculated in Equation 3.14.

$$P_{noise} = k_b \cdot T \cdot B = k_b \cdot 300 \cdot 7{\cdot}10^9 = 2.9{\cdot}10^{-11}\ \mathrm{W} = -75\ \mathrm{dBm} \tag{3.14}$$

3.5. RFID implementations

This section will describe different implementations of RFID systems that could be used. For each design, the working principle, a possible realisation, the expected performance and its feasibility for assisting sediment research will be discussed.

3.5.1. Regular chipped RFID

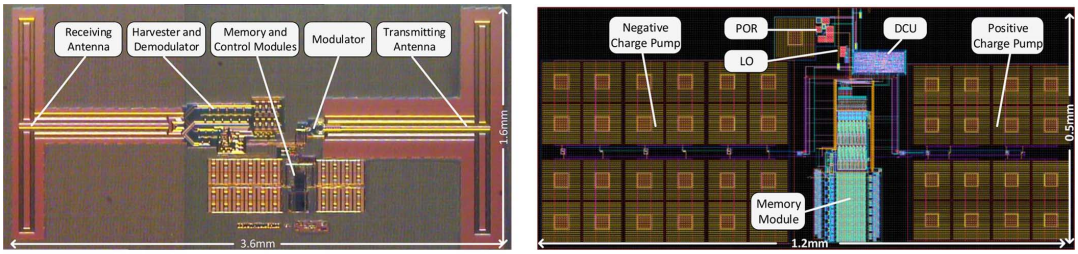

(a) (b)

Figure 3.1: One of the smallest chipped tags designed [18]

Very small chipped RFID tags have already been designed [18, 19] one of them is depicted in Figure 3.1. Both of these were made by using an antenna that was directly embedded on the silicon die. The disadvantage of this is that silicon is a semiconductor and thus has quite a lot of loss. These tags also tend to use impedance modulation of the antenna which will only function as a method of information transmission in the near field. These effects combined make that these tags have a short reading range [18, 19]. Producing the tags for testing is also a challenge as advanced silicon processing is needed. Tags like the one depicted in Figure 3.2, which already have been used for sediment research such as in [6], are too large for this research and also have a limited reading range.

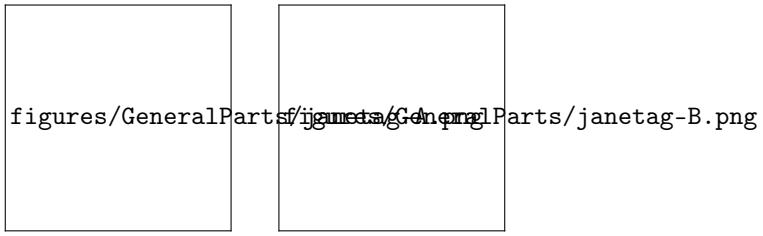

(a) Schematic drawing of the tag (b) Picture of the tag

Figure 3.2: A tag previously used in sediment research [6]

3.5.2. Radar reflector

A radar or corner reflector is already commonly used to make ships and buoys easier to see on radar systems. These reflectors only have a diameter of 30 cm, but still significantly increase the radar detectability of a yacht.

Figure 3.3 shows the structure that the radar reflectors are based on. Incoming waves enter one of the octants and are reflected three times off the three perpendicular surfaces, which reverses the direction of the wave back towards the transmitter, parallel to the incoming wave. This allows for the very high RCS of these structures relative to their size.

The reflectors will need to be encapsulated in a material that is penetrable for a specific frequency band and impervious to all other frequencies for them to be uniquely identifiable. This way, the other frequencies are scattered in all directions but the single band is reflected back to the receiver with a high gain.

For this implementation, the difficulty is in the encapsulation material as there are no materials available with a high enough quality factor for their filter characteristics [20].

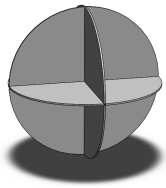

Figure 3.3: Render of the geometric structure of a radar reflector

3.5.3. Resonating Structure

A tag that is made of a resonating structure is an example of a passive, chipless, frequency coded design that has been discussed in section 3.3. Its main working principle is that an incident signal, often in the UWB-band, causes the tag to resonate on a certain frequency, similar to a tuning fork. This frequency response is then measurable at the receiving antenna.

A simple implementation is the use of microstrip dipoles with different lengths on a substrate as visble in Figure 3.4a [21]. The dipoles act as half-wave resonators, reradiating signals at different frequencies when incidented with a broadband pulse. By adding or leaving out one of the dipoles, bits can be encoded through the presence or absence of dips in the frequency domain. How this looks like can be seen in Figure 3.4b. For this particular implementation, five bits can be reached with five dipoles on a surface of 25×30 millimetres. The frequency range is between 5 to 6 GHz. One bit per 100 MHz bandwidth could be reached. When a 500 mW signal is transmitted, the maximum distance measured shows to be several tens of centimetres [22].

The main advantage of this tag is that it is extremely easy to make. They do not have to draw power from a battery and no semiconductor processes are involved. The drawback is that the range is restricted due to the limited amount of power that is radiated back.

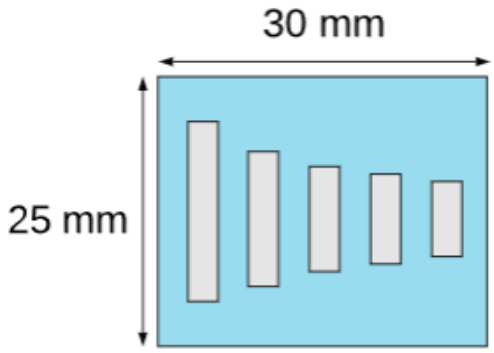

(a) The tag using dipoles of different lengths.

(b) Example S_{21} response of the tag. A dip in the frequency indicates the presence of a dipole with a certain resonance frequency.

Figure 3.4: Frequency encoded tag as described in [21].

3.5.4. Transmission Line Delay

As was discussed in the previous section, a chipless tag can also be encoded using the time domain. This is done by adding parasitic elements on a transmission line, resulting in a specific sequence of returning signals. An example of such a system is described in [23]. This particular design is visualised in Figure 3.5a and its lumped element model in Figure 3.5b. Evenly distributed capacitors along the line create impedance mismatches in the transmission line which create reflections. Placing or not placing a capacitor will create the possibility to encode one bit.

The tag in question has four bits on a board of 82×31 millimetres. The tag operates in the UWB frequency range and its maximum reading distance is calculated to be 56 centimetres.

A big disadvantage of these tags is their size. Each segment between a capacitor has to be at least 18 centimetres long to avoid temporal overlap. This makes miniaturisation very difficult. Its advantages are that the tag design is very simple and predictable, which makes it cheap and easy to design.

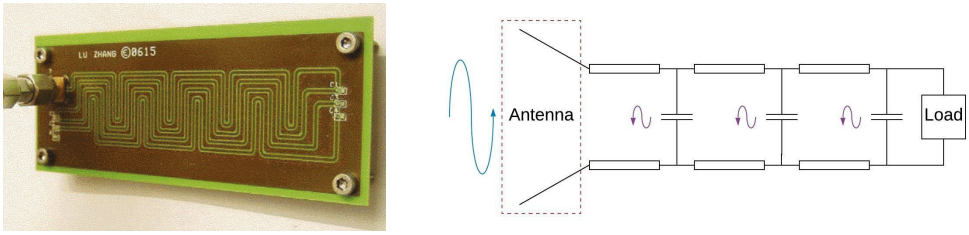

(a) A time encoded tag, as described in [23] (b) A lumped element model of a time encoded RFID tag

Figure 3.5: Time encoded RFID tags

3.5.5. Non-linear tag

As described in subsection 3.4.2, clutter can be significant when measuring UWB pulse responses. This will quickly cause the tag response to be buried in this background clutter. A solution is to have a tag that will contain a non-linear element in it that will create harmonics of the incoming signal [24]. These harmonics can still effectively be transmitted by the tag's antenna as the new wavelength will be a unit fraction of the old wavelength. The advantage of this frequency shift is that now the clutter is in a different frequency band than the tag response. This allows for the clutter to simply be filtered out and only the received noise matters as described in subsection 3.4.2.

These tags can be realised with a straight dipole antenna connected to a diode, but this will make them half as large as the wavelength of the used radio frequency. To keep the tags small, folded dipole structures can be considered, but these are more difficult to optimise and can still only be reduced in size 5 times as described in subsection 3.6.1. Figure 3.6 shows a folded dipole implementation.

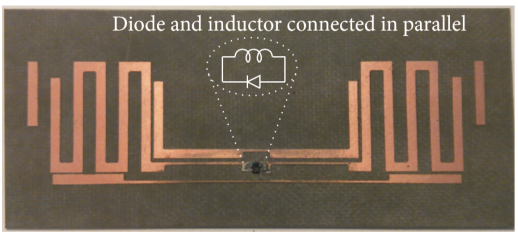

Figure 3.6: Folded dipole structure with a non-linear element as discussed in [24]

3.6. RFID antenna miniaturisation techniques

When a chipped tag is designed, the main part of the tag size is determined by the antenna. The size of an antenna design is mostly related to the wavelength it is tuned to. By folding the antenna, the size can be reduced to about a fifth of the wavelength [25]. For a 4 mm tag this would correspond to a tuning frequency of about 15 GHz, and such high frequencies would dramatically increase the amount of clutter coming back from the surface and no commercial RFID chips would be available for use.

3.6.1. High permeability magnetic core antenna

Another way to miniaturise antennas is to increase their effective aperture by using ferromagnetic (high permeability) materials [26]. This is a practice commonly found in long- to shortwave radios and more recently in low frequency RFID applications [6]. The reactive energy stored in the magnetic material might be used to create a separation in time or frequency domain between the received signal and surface clutter. Current

designs using this technique are much larger than the maximum specification in this project, see Figure 3.2. These tags also mostly operate in the near field and thus have a small reading range.

3.6.2. High electric permittivity materials

Another method to shrink antennas and resonators is to embed them in a high permittivity material. This is somewhat similar to using magnetic materials. The shorter wavelength in a high dielectric material makes it possible to shrink a given conductive structure while maintaining the same tuning frequency. A practise commonly used in mobile phone antennas [27], an example is shown 3.7.

Figure 3.7: Ceramic high permittivity antenna [28]

3.7. Choice of implementation

The designs discussed in section 3.5 are compared and evaluated in Table 3.2. After careful consideration, it was chosen to implement the system described in subsection 3.5.3. This is a chipless frequency encoded tag, which has a frequency dependent radar cross section. This method was chosen as it is easy to produce and prototype, has the potential to be created at the required sizes [29] and promises an adequate reading range [30].

Based on this design choice a system overview was created. This is visualised in Figure 3.8. For the sake of this project, this system was divided into three subsystems. For each subsystem a thesis is written. The system consists of the tag, transceiver hardware and signal processing. A detailed report on the tag design is written by [31]. In [32], the design of the transceiver hardware will be described. This mainly consists of the design of antennas. Measuring data is one thing, but interpreting is at least just as important. In [33], the signal processing system will be designed.

For the entire system, a preliminary calculation on reading distance was made using Equation 3.6. The worst case was assumed, given a frequency of seven gigahertz. The gain of the antennas was set to one, and a radar cross section σ_{RCS} of -60 decibel square meters. The transmitted power was set to be 32 Watt, and the power received -110 dBW. The maximum reading range was then derived to be 1.3 meters using Equation 3.15 from [30].

$$R = \sqrt{\frac{P_{tx,max} G_{tx} G_{rx} \lambda^2}{P_{rx} (4\pi)^3} \sigma} \tag{3.15}$$

Table 3.2: Implementation consideration table

	Bit density	Ease of manufacturing	Clutter sensitivity	Material availability	Power requirement
Chipped RFID	+	-	++	+	-
Radar reflector	0	+	+	- -	+
Resonating structure	0	++	0	0	0
Transmission line delay	-	-	0	+	-
Non-linear tag	-	0	+	+	-

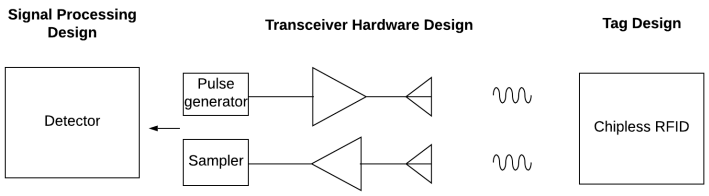

Figure 3.8: Overview of the system divided into three parts.

4

Digital system processing

This chapter of the paper will focus on aspects of the design that are confined to the sampling and processing of received signal. For further design an extended list was made for this section centred around the following design goal:

"Detecting a resonating tag and identifying the location".

To reach this goal a number of deliverables are identified.

- A signal generator whose output covers the UWB spectrum
- A measurement setup able to sample the UWB signal received by the antenna's.
- Software able to process the sampled signal with the goal of recognising a tag.

The design of each of these components and the choices made will be discussed in the upcoming sections.

4.1. Signal generation

Before one can measure the frequencies at which a chipless tags respond, a signal needs to be sent towards the tag to make it resonate. Because of the electrically linear behaviour of the tag this signal needs to contain all frequency components an arbitrary tag could resonate on. Two main signal types are available with this property: a chirp or frequency sweep, and a pulsed signal. For this design, the choice to go with the latter was made for two reasons. First off, due to the short nature of a pulse, clutter will only be received for a short time. The resonating late-time response of the tag the received signal from a tag can be separated from the clutter in the time domain, as discussed in subsection 3.4.2. A representation of this is shown in Figure 4.1, where the tag is able to be detected after the room response to the pulse has subsided. The second reason for using a pulse shape as transmitted signal is since lowering the repetition rate of the pulse allows the instant power to be increased while keeping the average power equal. This would create the opportunity to comply with the FCC regulations on transmitter power while having sufficient reading range.

4.2. Detection

After the pulse is emitted by an antenna and received by another antenna, it will need to be processed into a represenation from which tags can be identified. Since the proposed signal processing is done in the digital domain, first a look will be taken at sampling, after which detection methods are discussed.

4.2.1. Sampling

Since frequency components need to be detected throughout the UWB-spectrum, a sampler is required with a Nyquist frequency above 10.5 GHz, which is very fast and is not economically viable using real-time sampling.

An alternative to real-time sampling is stroboscopic sampling. In stroboscopic sampling the sampler records

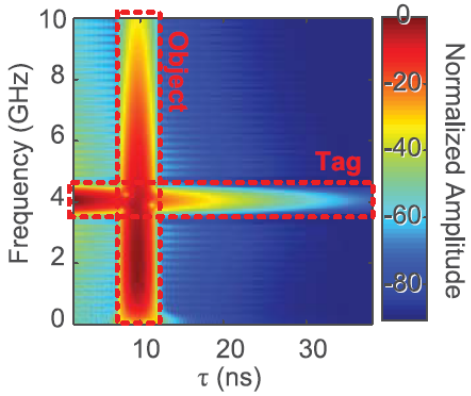

Figure 4.1: A frequency domain representation showing the difference between an scattering object and resonating tag *from: [34]*

samples as long as the repetition time of the signal. Now, when the sample rate of these samples isn't sufficient for the application, the trick employed in stroboscopic sampling is to take several samples but each with a different time shift.

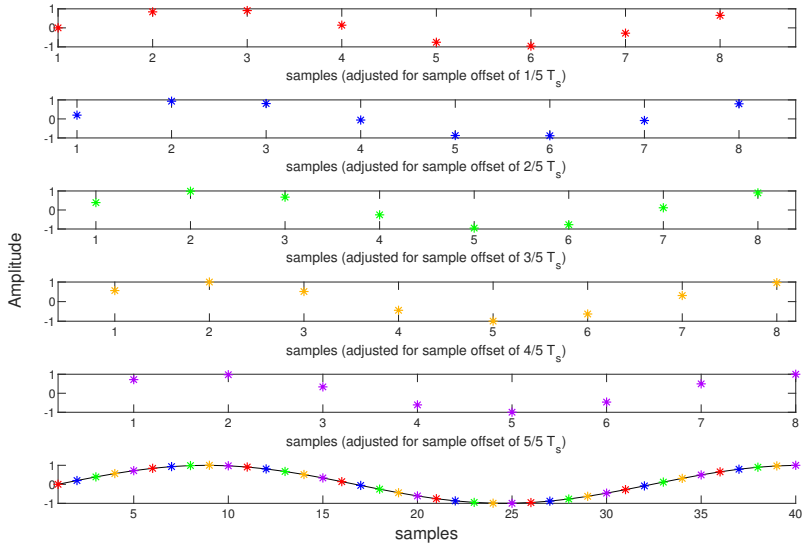

Figure 4.2: Set of plots to show the concept of stroboscopic sampling, combining the 5 samples in the first plots into the final plot

Figure 4.2 shows a simple implementation that visually gives insight into stroboscopic sampling. 5 samples are taken from a vector, each at 1/5 of the vector's virtual sample rate. As each of these series is sampled with a different offset that is a multiple of 1/5 the desired sample time, the 5 vector can be merged together to reveal the original sine wave.

To allow for the high speed, a trade-off is made to the accuracy per sample in bits. The accuracy is more commonly expressed as the dynamic range of the sampler, since it describes the ratio between the largest feature that can be detected before clipping occurs and the smallest feature that isn't lost to the rounding error of the ADC.

To sample the tag response effectively it needs to fill the dynamic range as much as possible. This, however, is not possible as the direct path between transmitter and receiver will be larger in amplitude. Attenuating this

response with an EM damping mat allows for the rest of the response to be further amplified and be sampled with a higher resolution.

4.2.2. Background suppression

For the best results in a static setup like the lab setup, a pair of identical measurements can be taken, one without and one with a tag in front of the receiver. The measurement without the tag can now be used as a reference for the signal with the tag present. The room response can be partially cancelled out, depending on how stationary the room is as well as the measurement errors.

Another technique that can be employed to improve SNR is to set the linearly polarised antennas up with their polarisations perpendicular to each other. This fully attenuates the direct path and reflections, only leaving the Rayleigh scattering part of the clutter and the tag response.

4.2.3. Tag detection

As described in **??** the signal component received from the tag will be of harmonic nature. A number of mathematical tools are available to determine of what frequency components a signal is built up. However, since the received signal is not harmonic throughout its duration, they cannot be directly applied. The following sections focus on a number of different approaches to extract the data from the received signal with the goal of recognising tag characteristics.

Fourier transform

The Fourier transform is a transform commonly used to represent a signal in frequency domain. Equation 4.1a and 4.1b show the mathematical representation for the time continuous and discrete functions respectively.

$$F(\omega) = \frac{1}{\sqrt{2\pi}} \int_{-\infty}^{\infty} f(t) \mathrm{e}^{-i\omega t} dt \tag{4.1a}$$

$$X[k] = \sum_{n=0}^{N-1} x[n] \mathrm{e}^{-i2\pi \frac{n}{N} k} \tag{4.1b}$$

The received signal can be processes using an accelerated implementation of the discrete Fourier transform like the radix method[35]. As described in[36], a derivation of the transform can be used to represent a signal in the time frequency domain, the short time Fourier transform. It slices the time domain signal into short segments and computes the Fourier transforms separately.

The advantage of a representation in time domain is that the short response from the tag does not get drowned whit in relatively high power clutter caused by surrounding objects. It does come however at he loss of resolution in the frequency domain. Figure 4.3 shows how the choice of signal length influences the certainty achieved in time and frequency domain.

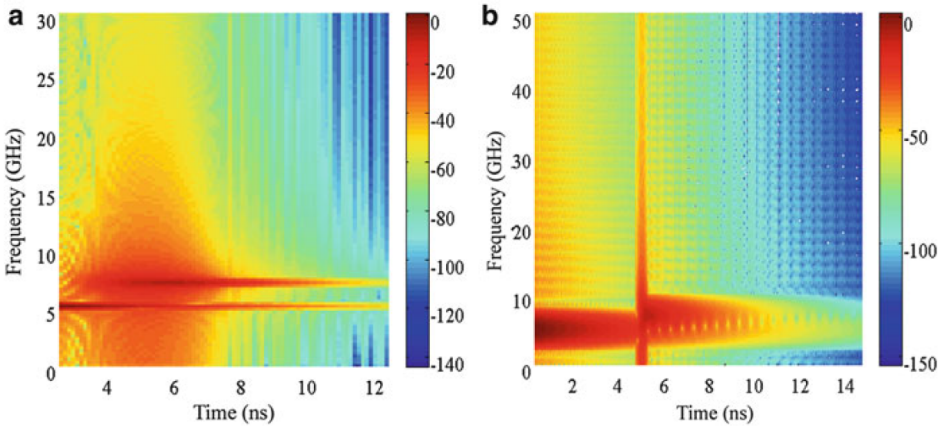

Figure 4.3: Spectrogram of the short time Fourier transform of a signal divided into lengths of (a) 5 ns (b) 0.64 ns *from: [37]*

Another effect to consider is the how the choice of window influences the resulting spectrum. Two figures of merit are used to judge the performance of window: the spectral leakage and time resolution.

Figure 4.4 shows a set of commonly used windows and their frequency response. Because the frequencies Will need to be detected for tags to be identified, a window with low spectral leakage is chosen, which will be the Hamming window.

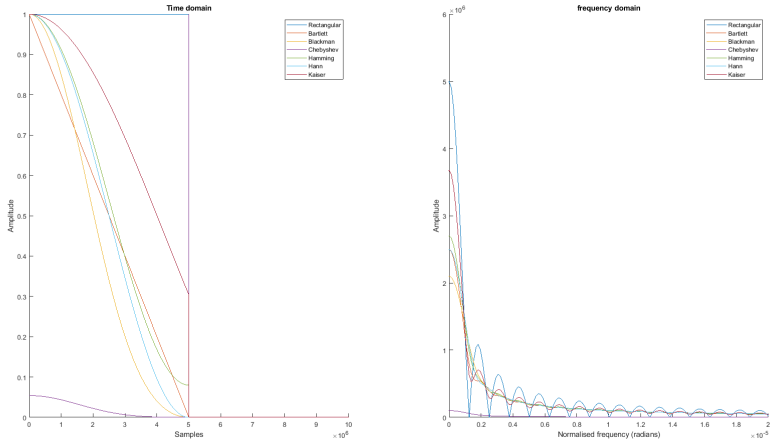

Figure 4.4: Time and frequency plots of common window functions

Matrix pencil method

The Matrix pencil method was developed with the goal to achieve a better trade off between time and frequency domain[37]. An input signal signal is given by Equation 4.2.

$$y(t_k) = \sum_{n=1}^{N} R_n {z_n}^k \tag{4.2}$$

with z_n given by:

$$z_n = e^{S_n \delta t} \tag{4.3}$$

The received signal is used to build matrices Y_1 and Y_2 given by Equation 4.4 and 4.5 for any $L < N-1$.

$$[Y_1] = \begin{pmatrix} y(0) & y(1) & \cdots & y(L-1) \\ y(1) & y(2) & \cdots & y(L) \\ \vdots & \vdots & \ddots & \vdots \\ y(N-L-1) & y(N-L) & \cdots & y(N-2) \end{pmatrix}_{(N-L)xL} \tag{4.4}$$

$$[Y_2] = \begin{pmatrix} y(1) & y(2) & \cdots & y(L) \\ y(2) & y(3) & \cdots & y(L+1) \\ \vdots & \vdots & \ddots & \vdots \\ y(N-L) & y(N-L+1) & \cdots & y(N-1) \end{pmatrix}_{(N-L)xL} \tag{4.5}$$

With Z_0 the diagonal matrix the N dominant poles of the input signal and R a diagonal matrix with their respective residues, the decomposition as in Equation 4.6 can be made.

$$[Y_1] = [Z_1][R][Z_2] \tag{4.6a}$$

$$[Y_2] = [Z_1][R][Z_0][Z_2] \tag{4.6b}$$

Where Z_1 and Z_2 are given by Equation 4.7 and Equation 4.7 respectively.

$$[Z_1] = \begin{pmatrix} 1 & 1 & \cdots & 1 \\ z_1 & z_2 & \cdots & z_M \\ \vdots & \vdots & \ddots & \vdots \\ {z_1}^{N-L-1} & {z_2}^{N-L-1} & \cdots & {z_N}^{N-L-1} \end{pmatrix}_{(N-L)xN} \tag{4.7}$$

$$[Z_2] = \begin{pmatrix} 1 & z_1 & \cdots & {z_1}^{L-1} \\ 1 & z_2 & \cdots & {z_2}^{L-1} \\ \vdots & \vdots & \ddots & \vdots \\ 1 & z_M & \cdots & {z_M}^{L-1} \end{pmatrix}_{NxL} \tag{4.8}$$

From the matrix pencil given by Equation 4.9 it can be seen that the values of z_i can be found by solving the eigenvalue problem given by Equation 4.10 [37].

$$[Y_2] - \lambda[Y_1] = [Z_1][R]\{[Z_0] - \lambda[I]\}[Z_2] \tag{4.9}$$

$$\{[Y_1]^+[Y_2] - \lambda[I]\} \tag{4.10}$$

For a noisy signal singular value decomposition can be used to filter out poles originating from that noise. To accomplish this first the matrix Y needs to be created as given in Equation 4.11. It can be seen that seen that matrices Y_1 and Y_2 can be derived form matrix Y by removing either the right or left-most column respectively.

$$[Y] = \begin{pmatrix} y(0) & y(1) & \cdots & y(L) \\ y(1) & y(2) & \cdots & y(L+1) \\ \vdots & \vdots & \ddots & \vdots \\ y(N-L-1) & y(N-L) & \cdots & y(N-1) \end{pmatrix}_{(N-L)x(L+1)} \tag{4.11}$$

Now singular value decomposition can be used find the singularities of the received signal.

$$[Y] = [U][\Sigma][V]^H \tag{4.12}$$

A filter parameter p is used to set a threshold value as given in Equation 4.13. Any singular value below the thresholds is set to zero, after witch the filtered version of matrices following Y_1 and Y_2 can be constructed Equation 4.14. Matrix Σ' is the filtered singular matrix and matrices V_1' and V_2' are the matrix V with the right and left-most column removed respectively [37].

$$\frac{\sigma_c}{\sigma_{max}} \approx 10^{-p} \tag{4.13}$$

$$[Y_1] = [U][\Sigma'][V_1']^H \tag{4.14a}$$

$$[Y_2] = [U][\Sigma'][V_2']^H \tag{4.14b}$$

Once the the poles of the received signal are found the corresponding residues can be found by solving Equation 4.15.

$$\begin{pmatrix} y(0) \\ y(1) \\ \vdots \\ y(N-1) \end{pmatrix} = \begin{pmatrix} 1 & 1 & \cdots & 1 \\ z_1 & z_2 & \cdots & z_M \\ \vdots & \vdots & \ddots & \vdots \\ {z_1}^{N-1} & {z_2}^{N-1} & \cdots & {z_N}^{N-1} \end{pmatrix} \begin{pmatrix} R_1 \\ R_2 \\ \vdots \\ R_M \end{pmatrix} \tag{4.15}$$

Just as was the case for the short time Fourier transform a time frequency representation can created by applying a sliding window to the received signal and calculation the set dominant poles for each set. This technique has proven itself to perform better is a noisy environment compared to the short time Fourier transform given that its parameters, the threshold and the window size, are able to be properly tuned

Frequency mixing
Frequency mixing is a technique based on the idea of band power detection. By multiplying an input signal with an sine oscillating at a frequency of interest the spectrum of the incoming signal is shifted by the same amount. Coincidentally the frequency of interest is now in baseband. By following this stage up with a low-pass filter and power detector the system is able to inspect specific segments of the spectrum for an increase in power which could point to the presence of a tag. The structural representation of the system is shown in Figure 4.5.

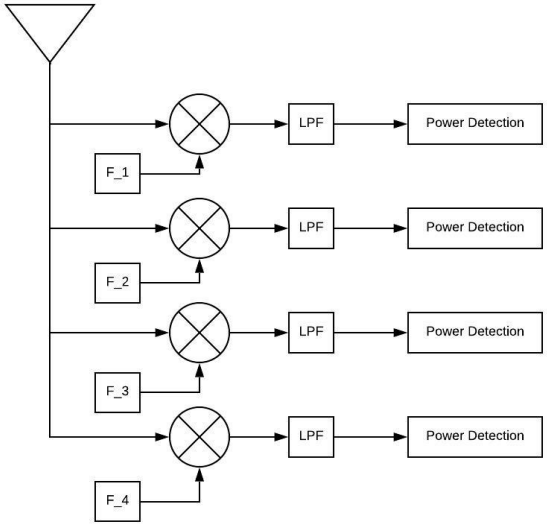

Figure 4.5: Structural design of frequency mixing power detector

4.2.4. Simulation
For a first test of the different detection systems, multiple cosine functions where added together and noise was added all using Matlab. From these simulations it can be seen that additive white Gaussian noise only prevents detection when the signal to noise ratio sinks below -15dB.

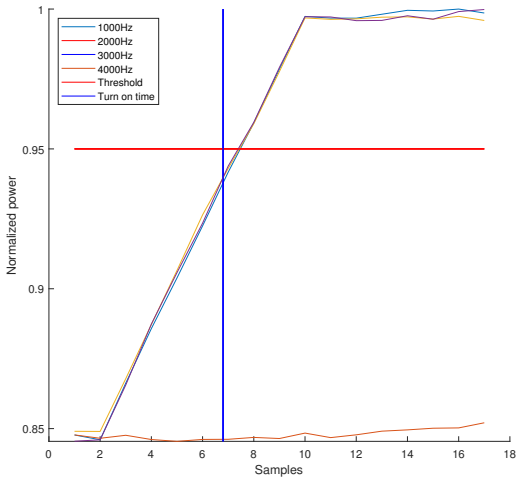

Figure 4.6: Simulation result of frequency detection using mixing on a -15dB SNR signal

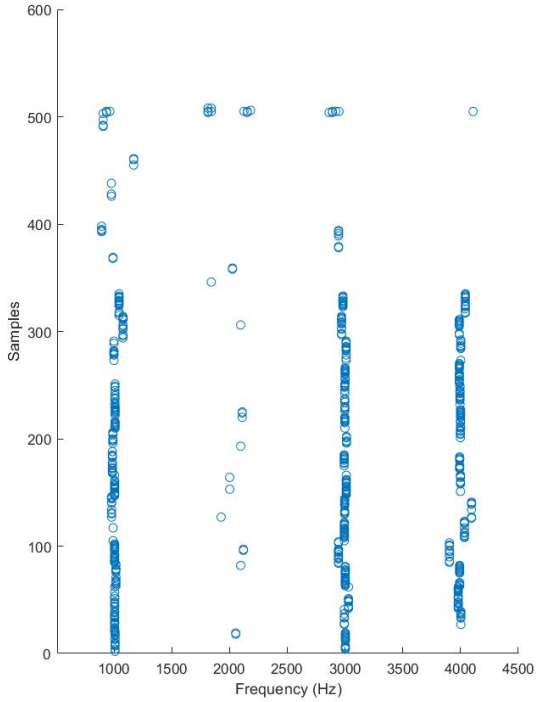

Figure 4.7: Simulation result of frequency detection using the short time Fourier transform on a -10dB SNR signal

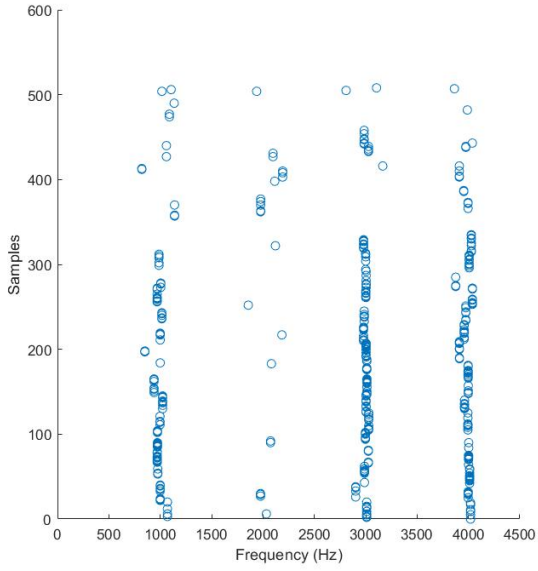

Figure 4.8: Simulation result of frequency detection using the matrix pencil method on a -10dB SNR signal

4.3. Lab setup

To evaluate the performance of the design the following lab setup was made. Figure 4.11 shows two different antennas used for testing. One of them is a high gain, high bandwidth antenna produced by Geozondas, the other one is the custom antenna designed by the antenna subgroup [32]. In both cases the antennas are facing an absorbing material in front of which a tag can be placed. This setup is shown in figure 4.10. This

figure also shows a schematic representation of the setup showing the connection of the pulse generator to the sampler and their connection to the respective antennas.

Figure 4.11 shows the two different types of tags used for testing. The first one are basic dipole resonating tags as described in [38]. Due to their proven design they allow us to validate our system and the benefits of depolarisation, without relying on the custom tags as designed by the respective subgroup [31].

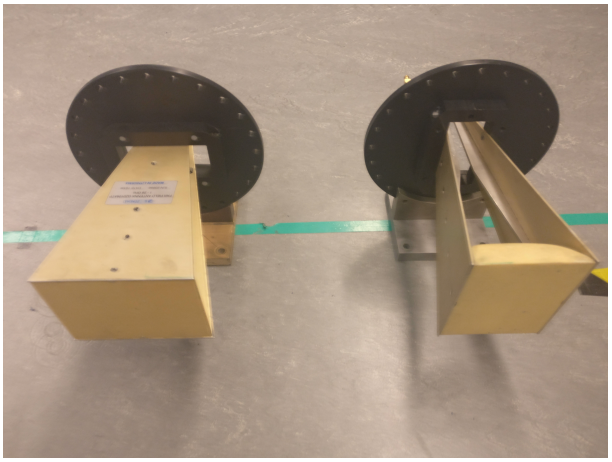

(a) High gain UWB antennas from Geozondas

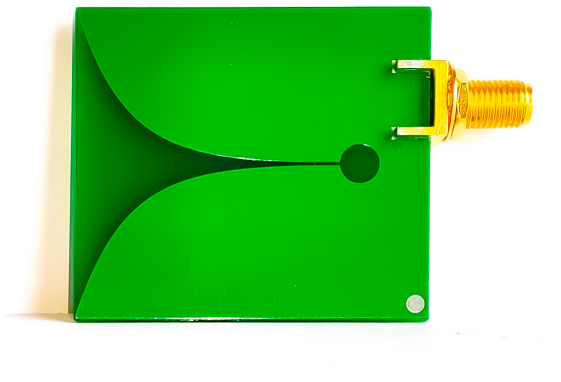

(b) Vivaldi antennas as designed by the antenna group [32]

Figure 4.9: Polarised antennas used for testing the RFID detection system

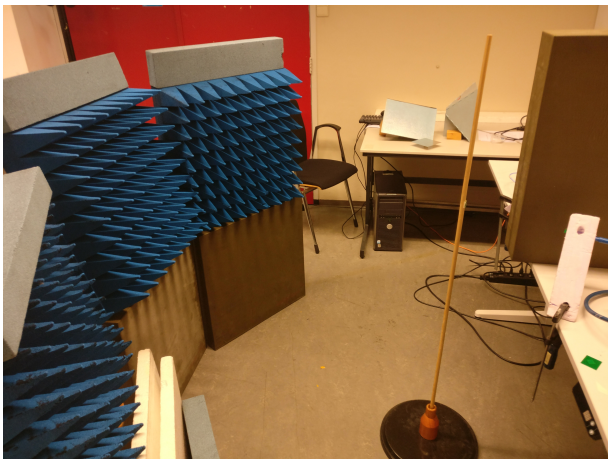

(a)

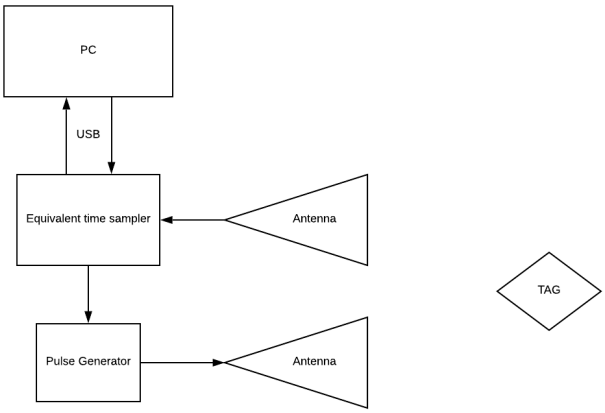

(b)

Figure 4.10: Measurement setup used to test the detection system

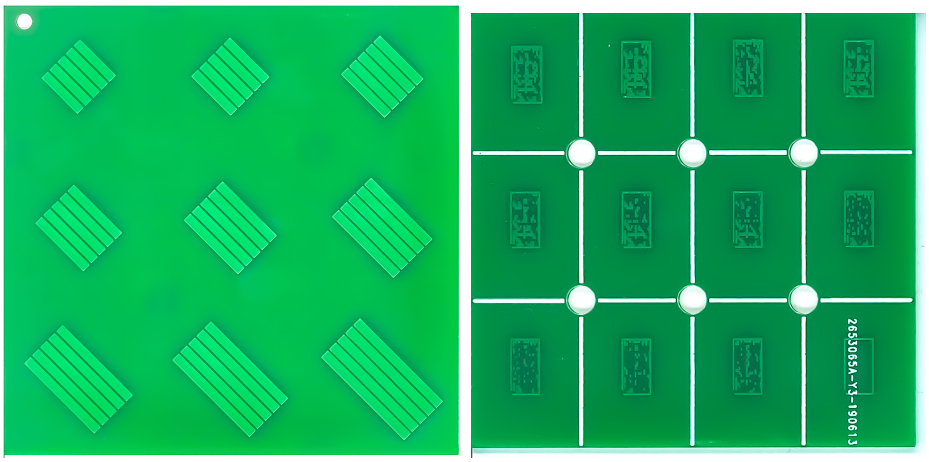

(a) Tags for testing (b) Tags as designed by the tag group [31]

Figure 4.11: 9 tags are manufactured on a PCB substrate at JLCPCB

4.4. Lab measurements and results

Initial testing was done with the custom tags. However, early testing didn't show any promise towards reliable detection as can be seen in Figure 4.12. The clutter power overpowers the signal from the tag in the early time and the tag does not seem to resonate for a long enough time to be detectable in late time.

For this reason the decision was made to order the additional batch of simple dipoles for validation of the detection system. A couple of different types of measurements were done for each of the tags. For each set of measurements a reference measurement was made with no tag placed in front of the antenna. The measurements are done in cross polarisation with the dipoles oriented at 45 deg relative to the polarisation of both the antenna's. Figure 4.14 and Figure 4.15 show the results obtained with the detection algorithms thus far. With the exception of the matrix pencil method the it can be seen that the peaks in power near the resonant frequency are being recognised all be it not with great accuracy. These results can be improved over time and by further optimising the filter functions used.

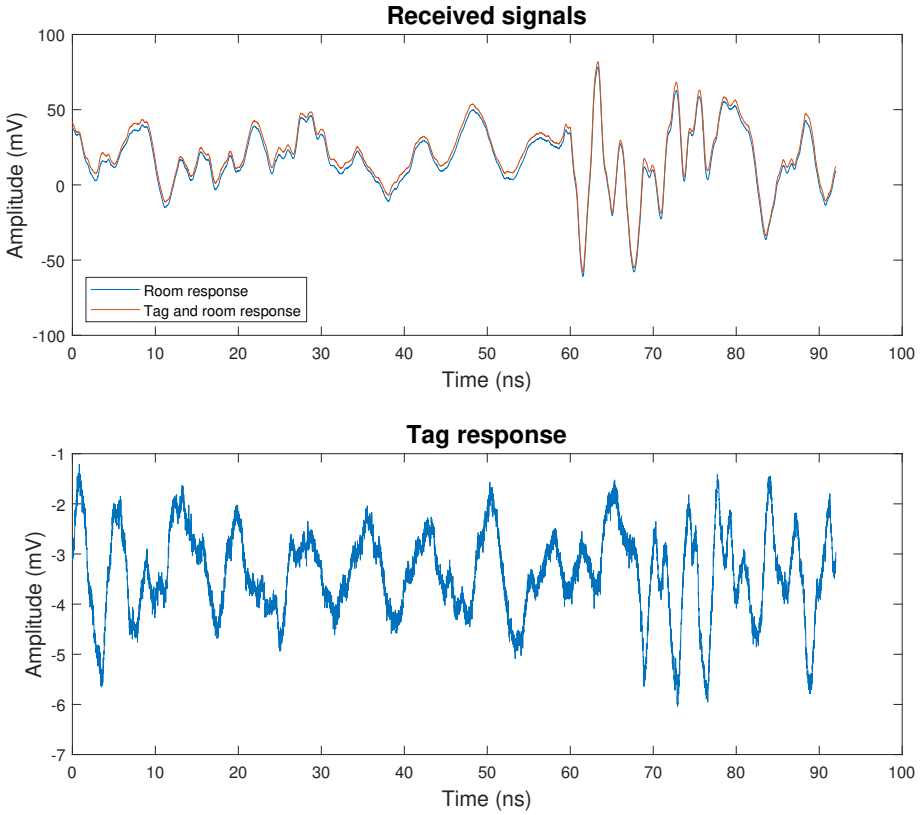

Figure 4.12: Time domain representation of the received signal of the tag as designed by in paper [31] coded at 5Ghz.

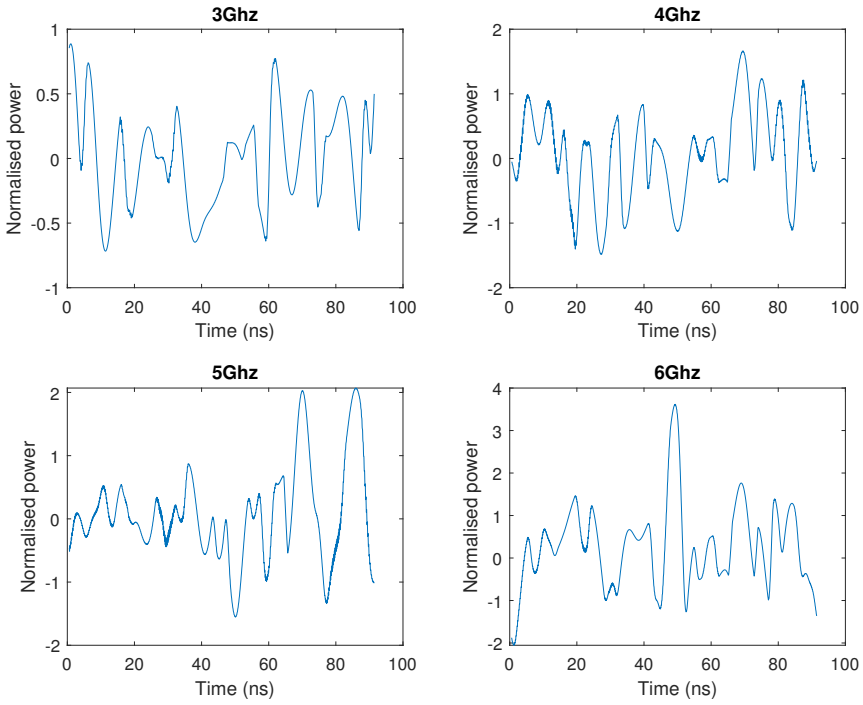

Figure 4.13: Application of the mixing method on the received signal of the tag as designed by in paper [31] coded at 5Ghz.

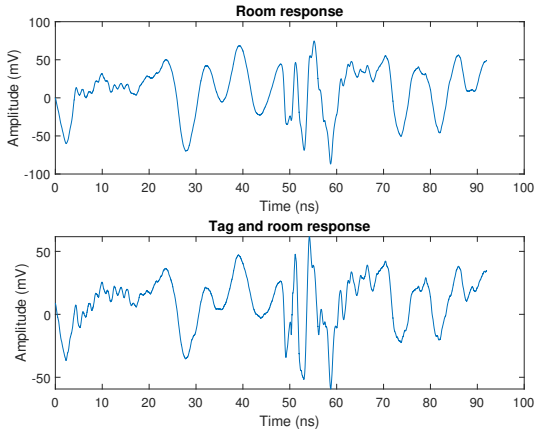

(a) Time domain signals a dipole with a 4.4Ghz resonant frequency

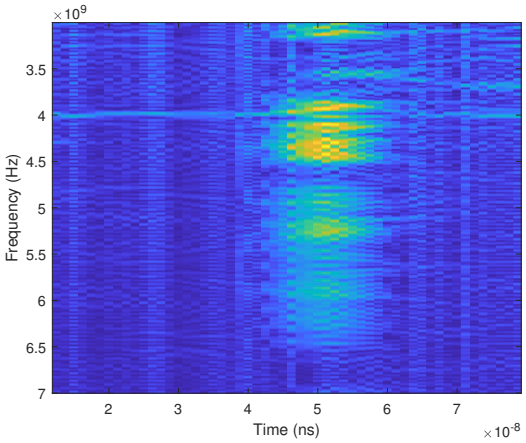

(b) Application of the STFT on the response of the 4.4Ghz dipole

Figure 4.14

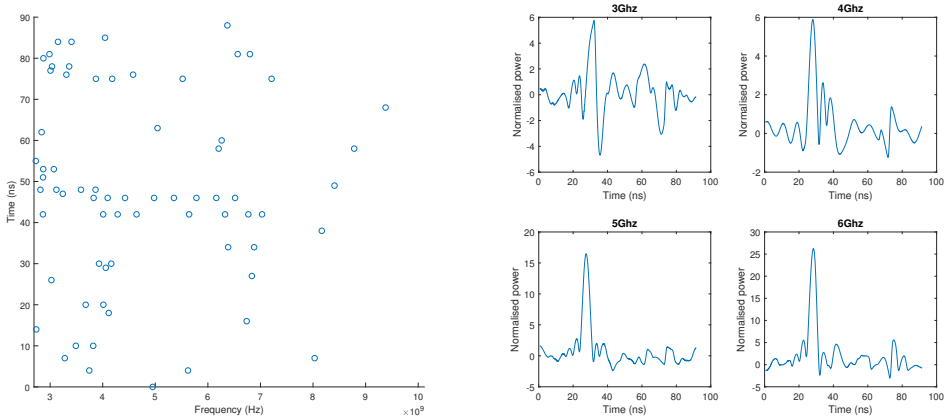

(a) (b)

Figure 4.15: Application of the matrix pencil method(left) and the mixing method(right) on a dipole with a 5Ghz resonant frequency

4.5. System Integration

Up until this point the main focus has been on designing the setup and software to be able to distinguish the signal reflected from the tag. In this section the focus will be on integrating the design into an application that allows a user to setup the system and select at which frequency tags should be detected. While driving the software and export the measurement to an .xlsx file. The frequencies can be coupled to a identifier, for example a number. This allows for a database to be updated after each rainy season that contains a list of GPS coordinates that specify the location of each tag each year.

Matlab was selected as platform due to its native support for matrix calculations and wide range of mathematical tools natively available. The app designer was used to create an application platform to easily test and employ the algorithms.

5

Discussion

As can be read in [33], the response of the system cannot yet be measured. It seems that the tag is either irresponsive or the signal is drowning in noise.

If the detection problem is due to the tag, several causes can be identified. First, it could be that the resolution of the realised tag is too low. When looked under the microscope, one can see that the corners of the tag are rounded off. It could be the case that these rounded corners change the structure so much, that their response is not comparable to the simulated response. This could, for example, mean that the tag's response is shifted to a frequency outside of the ultra-wideband. Another issue with the tag could be its substrate. The tag is printed on FR-4, which has increased losses in the gigahertz range. It was found that losses can be decreased by 20 percent if high frequency laminates like the Rogers 4000 series are used. This might be a significant improvement in the tag's response.

Except for the tag there are also some problems with the rest of the system, since the larger dipole tags could not be detected either. To have a better chance of detecting the tag, the signal-to-noise ratio has to be increased. This can be done by either minimising reflections or by transmitting a stronger signal. The pulse generator of the time domain sampler and the network analyser both do not output a lot of power. By placing an amplifier in the output path of these instruments, more energy will be pushed into the tags, possibly extending its response time. This could be the difference between seeing a tag and seeing noise. But, increasing the output power will also increase reflections.

The antenna polarisation isolation has been tested to be quite poor, especially at the higher frequencies. It it not sure whether this is due to the measurement setup or the actual values. To exclude one of these, a measurement should be done in an anechoic chamber.Besides this polarisation isolation measurement, it would be more precise if all measurement are done in an anechoic chamber, even though they may seem correct at first. This includes both the antenna measurements and the tag measurements, to minimise clutter. Unfortunately, this anechoic chamber was not available during the Bachelor's Thesis time window at the TU Delft.

6

Conclusion and Future Recommendations

In this thesis, a passive and chipless RFID system for sediment research is proposed. The system is intended to be deployed in Bolivia, where a semi-arid river with one source and one sink allows for the creation of a quantitative model where sediment particle size is related to bedload transport. This model requires individually distinguishable tags that reach the size of sand grains.

The designed tags use a Multiobjective Evolutionary Algorithm based on Decomposition combined with Enhanced Genetic Operators to miniaturise open-loop resonators with a fragmented base. Using this method, the tag reached a size of four by four millimeters. The designed tags operate in the ultra-Wide Band and have resonant frequencies between three and seven gigahertz. The quality factor of the optimised tags could reach approximately 130.

Antennas that are suited for use with ultra-wideband and provide a uniform phase center have been designed. The antennas have been tested to function correctly. Parameters such as the directivity and $S11$ parameter have been simulated and tested, and provide satisfying results. Some uncertainties remain about the polarisation isolation, but this requirement was stated to be of medium priority. Overall, the antennas are deemed to be suited for use in the electronic markers project.

During the final system testing, it was not yet possible to find the tags in the response produced by the test setup. It is not yet clear as why this is the case. No conclusions can be drawn yet because of this uncertainty: individual components are shown to work in simulations, and the antennas have been measured. Larger resonating tags have been tested and commercial antennas have been used. This still gave no decisive conclusion.

All in all, the project should not be considered a failure. Major progress has been made in the research of using RFID in sediment research. Although this implementation might not work, the alternative designs that are proposed in this thesis can be further explored.

Bibliography

[1] Ramon Batalla, Alison Collins, Heinz Glindemann, Sjoerd Hoornstra, Harald Köthe, Phil Owens, and John Quinton. The importance of sediment and sediment processes for river basin management. *European Sediment Research Network*, 2018. URL https://sednet.org/download/WG4_riverbasin.pdf.

[2] Chun Kiat Chang, Aminuddin Ab Ghani, Rozi Abdullah, and Nor Zakaria. Sediment transport modeling for kulim river – a case study. *Journal of Hydro-environment Research*, 2:47–59, 09 2008. doi: 10.1016/j.jher.2008.04.002.

[3] Kevin S. Black, Sam Athey, Peter Wilson, and Darren Evans. The use of particle tracking in sediment transport studies: a review. *Geological Society, London, Special Publications*, 274(1):73–91, 2007. ISSN 0305-8719. doi: 10.1144/GSL.SP.2007.274.01.09. URL https://sp.lyellcollection.org/content/274/1/73.

[4] Gema Guzmán, John Quinton, Mark Nearing, Lionel Mabit, and J Gómez. Sediment tracers in water erosion studies: Current approaches and challenges. *Journal of Soils and Sediments*, 13, 04 2013. doi: 10.1007/s11368-013-0659-5.

[5] Margot Chapuis, Christina J. Bright, John Hufnagel, and B.J. Macvicar. Detection ranges and uncertainty of passive radio frequency identification (rfid) transponders for sediment tracking in gravel rivers and coastal environments. *Earth Surface Processes and Landforms*, 39, 12 2014. doi: 10.1002/esp.3620.

[6] Bright, Christina Jane. Development of an rfid approach to monitoring bedload sediment transport and a field case study, 2014. URL http://hdl.handle.net/10012/8375.

[7] Klaus Finkenzeller. *RFID Handbook: Fundamentals and Applications in Contactless Smart Cards and Identification*. Wiley, third edition edition, 2010.

[8] Axel Decourtye, James Devillers, Pierrick Aupinel, François Brun, Camille Bagnis, Julie Fourrier, and Monique Gauthier. Honeybee tracking with microchips: a new methodology to measure the effects of pesticides. *Ecotoxicology*, 20(2):429–437, Mar 2011. ISSN 1573-3017. doi: 10.1007/s10646-011-0594-4. URL https://doi.org/10.1007/s10646-011-0594-4.

[9] Jiaguang Li, Stefan M. Luthi, Marinus Eric Donselaar, Gert Weltje, Maarten Prins, and Menno Bloemsma. An ephemeral meandering river system: Sediment dispersal processes in the río colorado, southern altiplano plateau, bolivia. *Zeitschrift für Geomorphologie*, 59, 12 2014. doi: 10.1127/zfg/2014/0155.

[10] A. Terry Bahill, B Bentz, and F F. Dean. Discovering system requirements. 01 2009.

[11] Jerry J Lou, Gary Andrechak, Michael Riben, and William H Yong. A review of radio frequency identification technology for the anatomic pathology or biorepository laboratory: Much promise, some progress, and more work needed. *Journal of pathology informatics*, 2:34, 08 2011. doi: 10.4103/2153-3539.83738.

[12] Y. A. Alshoudokhi, S. A. Alshebeili, M. A. Ashraf, M. R. AlShareef, and H. M. Behairy. Recent developments in chipless ultra-wide-band (uwb) radio frequency identification (rfid) systems. In *2017 IEEE 2nd Advanced Information Technology, Electronic and Automation Control Conference (IAEAC)*, pages 535–538, March 2017. doi: 10.1109/IAEAC.2017.8054072.

[13] N. C. Karmaker. Tag, you're it: Radar cross section of chipless rfid tags. *IEEE Microwave Magazine*, 17(7):64–74, July 2016. ISSN 1527-3342. doi: 10.1109/MMM.2016.2549160.

[14] C. Matzler. Microwave permittivity of dry sand. *IEEE Transactions on Geoscience and Remote Sensing*, 36(1):317–319, Jan 1998. ISSN 0196-2892. doi: 10.1109/36.655342.

[15] P. R. Lacko, W. W. Clark, K. Sherbondy, J. M. Ralston, and E. Dieguez. Studies of ground penetrating radar antennas. In *Proceedings of the 2nd International Workshop onAdvanced Ground Penetrating Radar, 2003.*, pages 24–29, May 2003. doi: 10.1109/AGPR.2003.1207287.

[16] Q. Wang, Z. An, Y. Yang, and C. Su. Emi principle and suppression method in vehicle ignition system. In *2012 Sixth International Conference on Electromagnetic Field Problems and Applications*, pages 1–4, June 2012. doi: 10.1109/ICEF.2012.6310311.

[17] Christian Ho, Stephen Slobin, Anil Kantak, and Sami Asmar. Solar brightness temperature and corresponding antenna noise temperature at microwave frequencies. *Interplanetary Network Progress Report*, 11 2008.

[18] H. Dagan, A. Shapira, A. Teman, A. Mordakhay, S. Jameson, E. Pikhay, V. Dayan, Y. Roizin, E. Socher, and A. Fish. A low-power low-cost 24 ghz rfid tag with a c-flash based embedded memory. *IEEE Journal of Solid-State Circuits*, 49(9):1942–1957, Sep. 2014. ISSN 0018-9200. doi: 10.1109/JSSC.2014.2323352.

[19] A. Y. Jou, H. Shan, H. Pajouhi, J. Peterson, and S. Mohammadi. A single-chip wireless powered rfid antenna and transceiver. *IEEE Journal of Radio Frequency Identification*, 1(3):219–227, Sep. 2017. ISSN 2469-7281. doi: 10.1109/JRFID.2017.2789246.

[20] D. Micheli, A. Vricella, R. Pastore, and M. Marchetti. Synthesis and electromagnetic characterization of frequency selective radar absorbing materials using carbon nanopowders. *Carbon*, 77:2326–2337, June 2014.

[21] I. Jalaly and I. D. Robertson. Capacitively-tuned split microstrip resonators for rfid barcodes. In *2005 European Microwave Conference*, volume 2, pages 4 pp.–1164, Oct 2005. doi: 10.1109/EUMC.2005.1610138.

[22] Romain Siragusa Pierre Lemaître-Auger Olivier Rance, Etienne Perret. *RCS Synthesis for Chipless RFID: Theory and Design*. Elsevier, first edition edition, 2017.

[23] Lu Zhang, S. Rodriguez, H. Tenhunen, and Li-Rong Zheng. An innovative fully printable rfid technology based on high speed time-domain reflections. In *Conference on High Density Microsystem Design and Packaging and Component Failure Analysis, 2006. HDP'06.*, pages 166–170, June 2006. doi: 10.1109/HDP.2006.1707587.

[24] Kimmo Rasilainen and Ville V. Viikari. Transponder designs for harmonic radar applications. *International Journal of Antennas and Propagation*, 2015, May 2015.

[25] G. Marrocco. The art of uhf rfid antenna design: impedance-matching and size-reduction techniques. *IEEE Antennas and Propagation Magazine*, 50(1):66–79, Feb 2008. ISSN 1045-9243. doi: 10.1109/MAP.2008.4494504.

[26] H. Wheeler. Small antennas. *IEEE Transactions on Antennas and Propagation*, 23(4):462–469, July 1975. ISSN 0018-926X. doi: 10.1109/TAP.1975.1141115.

[27] T. K. Lo, Chun-On Ho, Y. Hwang, E. K. W. Lam, and B. Lee. Miniature aperture-coupled microstrip antenna of very high permittivity. *Electronics Letters*, 33(1):9–10, Jan 1997. ISSN 0013-5194. doi: 10.1049/el:19970053.

[28] Hanna Kähäri, Prasadh Ramachandran, Jari Juuti, and Heli Jantunen. Room-temperature-densified li2moo4 ceramic patch antenna and the effect of humidity. *International Journal of Applied Ceramic Technology*, 14(1):50–55, 2017. doi: 10.1111/ijac.12615. URL `https://ceramics.onlinelibrary.wiley.com/doi/abs/10.1111/ijac.12615`.

[29] L. Wang, T. Liu, J. Sidén, and G. Wang. Design of chipless rfid tag by using miniaturized open-loop resonators. *IEEE Transactions on Antennas and Propagation*, 66(2):618–626, Feb 2018. ISSN 0018-926X. doi: 10.1109/TAP.2017.2782262.

[30] A. Vena, E. Perret, B. Sorli, and S. Tedjini. Theoretical study on detection distance for chipless rfid systems according to transmit power regulation standards. In *2015 9th European Conference on Antennas and Propagation (EuCAP)*, pages 1–4, April 2015.

[31] D.A.E. de Gruijl and M. Kraaijeveld. Electronic markers for geological research: Tag design. Technical report, Delft university of technology, 2019.

[32] A.S. Roos and M.A Postma. Electronic markers for geological research: Transceiver hardware design. Technical report, Delft university of technology, 2019.

[33] D. de Groot and E. van der Meijs. Electronic markers for geological research: Signal processing. Technical report, Delft university of technology, 2019.

[34] A. Ramos, E. Perret, O. Rance, S. Tedjini, A. Lázaro, and D. Girbau. Temporal separation detection for chipless depolarizing frequency-coded rfid. *IEEE Transactions on Microwave Theory and Techniques*, 64 (7):2326–2337, July 2016. ISSN 0018-9480. doi: 10.1109/TMTT.2016.2568180.

[35] I. J. Good. The relationship between two fast fourier transforms. *IEEE Transactions on Computers*, C-20 (3):310–317, March 1971. ISSN 0018-9340. doi: 10.1109/T-C.1971.223236.

[36] H. V. Sorensen and C. S. Burrus. Efficient computation of the short-time fast fourier transform. In *ICASSP-88., International Conference on Acoustics, Speech, and Signal Processing*, pages 1894–1897 vol.3, April 1988. doi: 10.1109/ICASSP.1988.196996.

[37] Reza Rezaiesarlak and Majid Manteghi. *"Chipless RFID Design Procedure and Detection Techniques"*. "Springer", "2015". doi: 10.1007/978-3-319-10169-9.

[38] A. Vena, E. Perret, and S. Tedjni. A depolarizing chipless rfid tag for robust detection and its fcc compliant uwb reading system. *IEEE Transactions on Microwave Theory and Techniques*, 61(8):2982–2994, Aug 2013. ISSN 0018-9480. doi: 10.1109/TMTT.2013.2267748.

Glossary

BAP Bachelor Graduation Project

EM electromagnetic

GPS global positioning system

IC integrated circuit

mmW millimeter-wave

plane wave approximation An approximation of (electromagnetic) waves which is valid when a wave source is far away and does not encounter small objects in comparison to the wavelength

RCS radar cross-Section

REE rare earth elements

RFID Radio-Frequency Identification

TDR time-domain reflectometry

UWB Ultra-wideband: term to describe radio communications systems that utilises a large bandwidth, usually more than 50% of the center frequency